Y/AMT-621

Y-12

OAK RIDGE
Y-12
PLANT

LOCKHEED MARTIN

Final CRADA Report
for
CRADA Number Y-1295-0354

PRODUCTION OF TESTING OF LASER CRYSTALS

Tom Schmidt
Lockheed Martin Energy Systems, Inc.
Allen R. Geiger
LaSen, Inc.

January 21, 1999

Approved for Public Release;
distribution is unlimited.

Prepared by the
Oak Ridge Y-12 Plant
managed by
LOCKHEED MARTIN ENERGY SYSTEMS, INC.
for the
U.S. DEPARTMENT OF ENERGY
under contract DE-AC05-84OR21400

MANAGED BY
LOCKHEED MARTIN ENERGY SYSTEMS, INC.
FOR THE UNITED STATES
DEPARTMENT OF ENERGY

UCN-13672 (2 11-97)

I. Abstract

Lasers and nonlinear optical systems are being developed to allow the construction of all solid state lasers with tunable output in the mid-infrared (3-5 μm). In these systems potassium titanyl phosphate (KTP) and its analogs (KTA, RTA and CTA) are used to construct Optical Parametric Oscillators (OPOs). In the past, large (5 mm × 5 mm × 15 mm) crystals of KTA, RTA and CTA have been difficult to obtain, and were costly as well. Also, the arsenate materials were limited in spectral range due to an AsO_4 overtone in the 3.5 to 5.0 μm region. There has also been interest in materials which self-OPO. This process is done by doping nonlinear materials with lasing ions.

This effort investigated the development of mixed metal analogs of KTA, which would lase and also suppress the AsO_4 absorption overtones to allow more efficient mid-infrared OPO operation.

II. Program Objectives

The primary objective was to investigate mixed metal doping of KTA type materials. This primary objective was to produce and evaluate these materials for phenomenon such as follows:

A. Analogs of KTP/KTA

B. Enhanced infrared transmission in KTA

C. Lasing ion doped KTA

III. Objectives Met Summary

Given the objectives listed in 2.0, the results are as follows:

3.1 Antimony analysis of KTP

Attempts were made to produce crystals of antimony and tellurium, notably potassium titanyl tellurate (KTT) and potassium tytanyl stibnenate (KTSb). The results were that both KTT and KTSb did not produce crystalline structures in the environments typically used to grow KTP and KTA.

3.2 Enhanced Transmission in KTA

Mixed metal doping of KTA did enhance the transmission of KTA in the 3.3 μm to 5.1 μm infrared region.

3.3 Lasing Ion Doped KTA

KTA was successfully doped with neodymium (Nd), ytterbium (Yb) and a mix of Nd and Yb. Doping levels of Nd were too low to be useful as a lasing material. Yb doping levels were good and stimulated cross-sections were at levels that indicate lasing action at 972 nm may be obtainable. Co-doping with Nd:Yb may enhance the overall efficiency of the Yb lasing action by metal to metal transfer of pump energies.

Attempts to dope KTA with holmium (Ho) and Thulium (Tm) met with limited success in that although Ho and Tm were incorporated into the KTA crystalline matrix, the lasing properties of these ions at room temperature are not suitable for general laser work.

IV. DOE Benefits

The crystalline materials developed in this program will be used to construct frequency agile lasers in the 1.3 μm to 4.0 μm region. Such lasers will be utilized in lidar remote sensors for site clean up, chemical weapon and treaty verification. These lasers are capable of producing multi-laser lines simultaneously, and as such, can be used to construct photo-activated high speed switches to trigger explosives.

V. Technical Discussion

The primary objective of the doping program was to dope KTA with lasing rare earth ions. It would appear that there is no site in KTA to substitute an ion as large as neodymium. Direct substitution of the rare earth ions is not possible. This lead research efforts to investigate the structural details of metal ions in KTA.

In order to understand better the mechanisms of the impurity incorporation into KTA lattice, it is useful to examine once more the KTA (KTP) structure. The structure of the KTA unit cell was determined reliably in by researchers (Northrup et al and S.C. Maja et al). Positions

of atoms given in these independent papers partially coincide with one another. The KTA (TP) structure was analyzed based on consideration of the following aspects:

a. Relative location of X and Y chains AsO_4 tetrahedron, TiO_6 octahedron, etc.
b. interchange of long and short Ti-O bonds in O-Ti-I-Ti...-chains
c. turns of tetrahedrons and octahedrons relative to the unit cell axes,
d. length of As-O, Ti-O and K-O bonds,
e. differences in positions of cations in pairs as As_1, and As_2, Ti_1, and Ti_2, K_1, and K_2, etc.

Such analysis is necessary and useful to understand the nonlinear properties of KTA. However, it is insufficient for understanding the peculiarities of potassium ion replacement by other ions. Thus we shall analyze KTA structure considering structure and packing of flat nets of oxygen atoms. Such an approach allows one to understand the details of potassium atoms coordination and the laws of their replacement by other ions. Besides, we shall consider the chemical aspects of K^+ replacement by other cations of various valences.

Analysis of KTA structure shows the most regular flat oxygen nets are located in (210) and (2-10) planes. The structure of oxygen net in the 210 plane is given in Figure 1. It is formed by tapes of 348 + 338 + 3838 (4:3:3) net, which are divided by Z-pores. Inside this tape there are closed eight membered rings, stretched along Z. They contain two knots. In the first knot (K-knot) there is a K^+ ion at certain polarity of the KTA cell. In the other knot (B-knot) the K^+ ion at reverse cell polarity is likely to be located. Actually, the B-knot can be considered as a K^+ vacancy, since in polydomain samples K^+ ions are located in K-knots in one type of domain, and in B-knots in another domain. Distance between K and B knots is small and equal approximately to 1.7 Å at room temperature. When increasing the temperature K and B knots are coming nearer each other (according to Northrop et al). At the side relative to the tapes (or of the Z pores) there are unclosed eight membered rings (Figure 1), which also contain K and B knots. These knots supplement the oxygen net up to the closest 3^6 one.

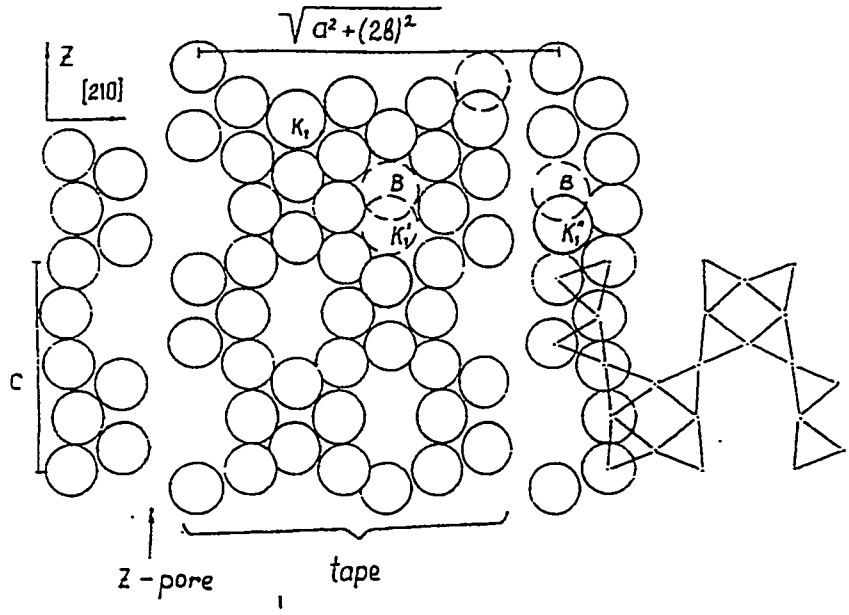

Figure 1. Oxygen nets of KTA in a (210) plane

The Z-pore destroys the net's order so that opposite to the unclosed 8-membered ring (half ring, consisting of 5 oxygen atoms) are located two oxygen atoms, which do not come into contact with the last atoms of the half ring (Figure 2). From the Figure 2, one can conclude that K'_1 and K''_1 ions have different coordination environments. However this is not so.

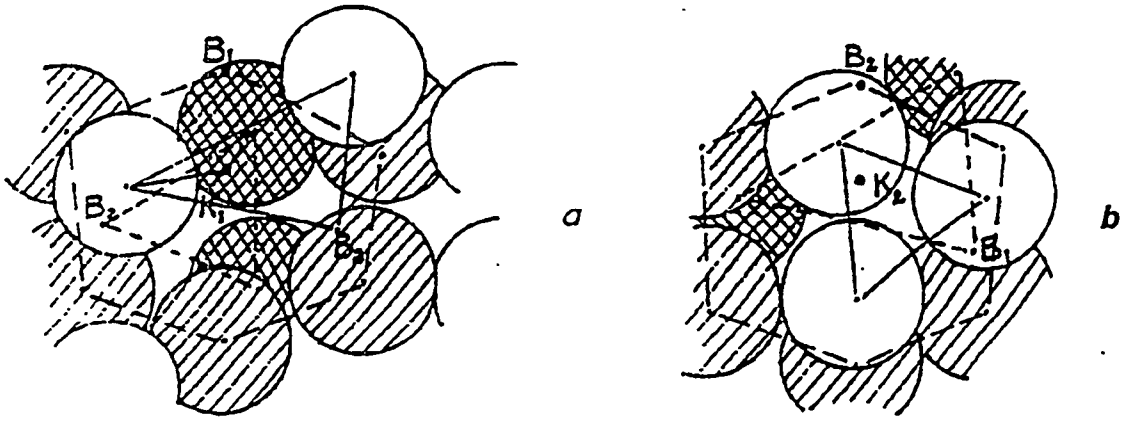

Figure 2. Coordination environment of K^+_1 (a) and K^+_2 (b) ions

Almost perpendicular to these nets (namely at an 89.94° angle) there are oxygen nets in the 2-10 plane which have the same structure. The combination of 210 and 2-10 is arranged in the way that the K'_1 knot in (210) is in a closed ring, while in (2-10) it is located in an unclosed ring at the side relative to the tape or to a Z-pore. The K" knot in (210) is in an unclosed ring at the side relative to the tape, while in (2-10) it is located in a closed ring. As a result, the coordination environments of K'_1 and K''_1 become similar, but turned relative to each other.

The potassium ions are known to have two different coordination positions. A 210 net in Figure 2 contains only K^+_1 (as denoted by Northrup et al). Above and below the net, given in Figure 2, there are 210 oxygen nets which contain K^+_2. These nets are similar, but one is shifted relative to the other. Their structure is the same as for a net with K^+_1, but positions of oxygen ions are a little different than for their analogues in the net with K^+_1. The displacement value varies from 0.01 Å to several tenths of an Å for various atoms. The oxygen 2-10 nets also are of two types. One type contains K^+_1, while the other has K^+_2. The 210 and 2-10 nets with K^+_1 are equivalent as in the case of 210 and 2-10 nets with K^+_2. Namely this equivalence gives the 90° angle between X and Y, which corresponds to orthorhombic symmetry of KTA cells.

Now let us consider the position of potassium ions in a KTA structure in detail. To date, they were supposed to have a coordination number of 9 because in the case of K_1 one oxygen is strongly remote and is not taken into account. From Figure 3a it is seen that in reality the K_1 environment is a distorted hexagonal cubo-octahedron. Both bases of trigonal prism of the cubo-octahedron include two oxygen atoms and B knots, relating to K^+_2. The 6-membered ring of cubo-octahedron consists of 5 oxygen atoms and of a B knot. It can be noted that distances between K^+_1 and each of two oxygen atoms in the prism base (see Figure 2a) are considerably shorter than other distances between K^+_1 and each of two oxygens, or two vacancies. Thus the K^+_1 coordination polyhedron can be simply considered as a hexagonal dipyramid, consisting of seven oxygen atoms and of a B-knot. The coordination environment of K^+_2 is shown in Figure 3b. It is a cubical cubo-octahedron. As in the K^+_1 case, the 6-membered ring around K^+_2 consists of 5 oxygen atoms and a B-knot. As in K^+_1 case, one base of the stretched octahedron consists of two oxygens and a B-knot, which as adjacent to K^+_1. However, the second base of the

octahedron consists of three oxygen atoms, which differ from the K^+_1 environment by large stability.

It is also necessary to consider the structure of X and Y chains...-tetrahedron - octahedron - etc. from the taken point of view. In Figure 3a, the Y chain is given in a schematic way. It is seen that positions of oxygen atoms along a Y-chain correspond to the simplest two-layer hexagonal ABA packing.

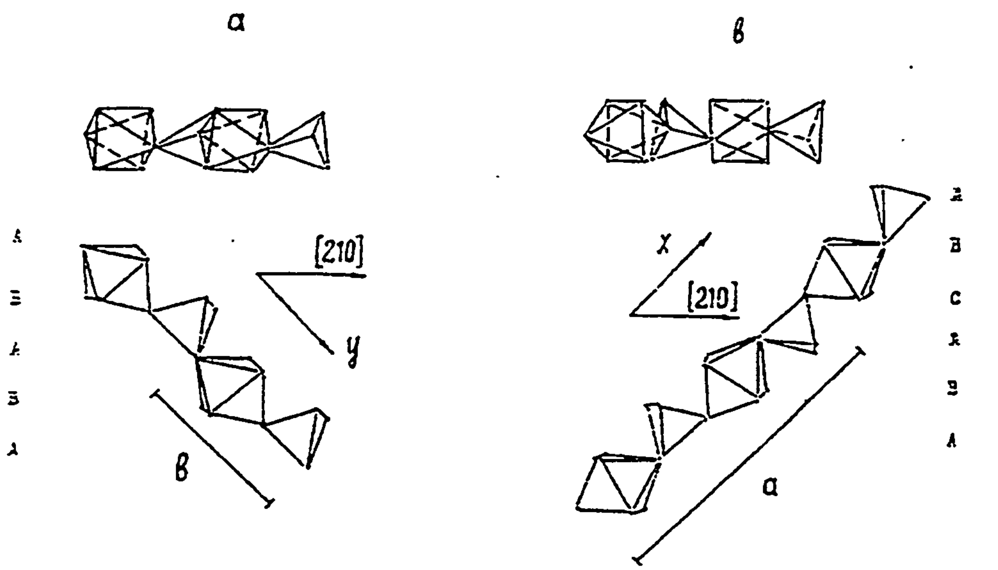

Figure 3. Packing of Y-chains (a) and of X-chains (b)

In Figure 3b the X chain is given. In this case packing of oxygen atoms corresponds to four layer hexagonal ABACA packing. It is seen that one TiO_6 octahedron has a normal form, while another is distorted. In reality, both octahedron are similar, but the first octahedron has a normal look in a 210 plane and a distorted one in a 2-10, while the second is distorted in (210), but is of normal appearance in (2-10). Such structure of X-chain brings to a smaller α period relative to 2**b**, and to stronger stresses in X-chains than in Y ones. Thus the X-chain is less stable than the Y-chain from the point of view of oxygen atoms packing.

Let us compare the structure of X and Y chains with an environment of K^+ ion. The K^+_1 is on the cross of Z pore and of X-pore. The X-chains has a complex four-layer packing, and the

K^+_1 environment is a middle one between a hexagonal cubo-octahedron and a hexagonal dipyramid. K^+_2 is on the cross of Z-pore and Y-pore. The Y-chains are ascribed into a simple two-layer packing, and the K^+_2 environment is a cubical cubo-octahedron. From the point of view of structure stability, both the K^+_1 and X-chain are less stable than the K^+_2 environment and the Y-chain. Further we shall see that it coincides with the experimental data.

In the paper by Northrup et al, the average K_1-O and K_2-O distances are 2.972- and 2.970 Å, respectively. Our calculation for a 12 coordination environment gives values which are only ~0.1 Å larger. If one were to take the O^{2-} radius as 1.32 Å, then the K^+ radius will be 1.7 Å. It is considerably larger than the standard K^+ ionic radius. And as a result, K^+ is easily replaced by monovalent ions up to a large Cs^+.

One can expect that such large coordination K^+ volume is to allow the easy K replacement by many cations, including Nd^{3+}. However, it is clear that the extent of potassium replacement for non-isovalent ions is to be strongly dependent on mechanisms of charge compensation. Thus it is necessary to consider the chemical aspect of K^+ replacement of ions of other valences.

The K^+ replacement by bivalent ions occurs easily enough. In particular, we found that Ba^{2+} which is the heaviest bivalent ion, can easily replace up to 2 mol% of K^+ and more. When replacing K^+ by a bivalent ion, the charge compensation may be realized in three ways. The first way is to form a K vacancy when two K^+ ions are replaced by one Ba^{2+}. The other way is a compensation of surplus positive charges by a titanium vacancy and/or by vacancies of titanium and oxygen which corresponds to $2Ba(2+) \rightarrow K_2TiO^{4+}$. And the third way is realized with participation of arsenic and oxygen vacancies as $Ba^{2+} \rightarrow KasO_2^{2+}$ replacement. Using the electro-optical techniques, we found that KTA samples doped by Ba^{2+} are monodomain crystals. When considering the filling of K- and B- positions by K ions, we can suppose which type of replacement should lead to growth of monodomain of KTA crystals.

As it was noted above in monodomain samples, all the potassium ions are located on one side of Z-axis, while the B knots are on the other one. Let us replace a B knot by K^+_1, for example. It is a disadvantageous in terms of packing energy because in this case the shifted K^+_1 will push off the nearest K^+_2 located in the same Z pore. Initially the K_1-K_2 distance was 4.44 Å, but became 3.19 Å. We can move all K^+ ions of one Z-pore to the place of B knots. It will

conserve the energetics of potassium ion's interaction with a Z-pore. However, in this case distances from moved K ions to potassium ions in adjacent Z-pores decrease from 4.44 Å to 4.16 Å, which is also energetically disadvantaged.

We can cut the KTA structure perpendicular to Z-axis and move all the K ions above the singled out plane to the place of B knots. In this case the marked out plane appears to be in the middle of a layer of B knots. It will be charged negatively relative to the whole crystal, and will be a domain wall. The energy of domain reorientation is known to be a very low- energetic process, but it cannot occur spontaneously. At the high temperature of KTA crystal growth the potassium ions are mobile and can take the more energetically advantageous monodomain state (for perfect crystals). Only defects can anchor the domain walls. Indeed, in V.D. Kugal et al's paper, formation of domains in initially monodomain samples was shown to occur at a high temperature after accumulating some amount of oxygen and potassium vacancies.

Let us return to discussion of K^+ replacement by Ba^{2+}. From the above analysis, it is clear that $2K^+$ replacement by Ba^{2+}, resulting in potassium vacancies formation, must also bring a polydomain character of KTA. We did not find this phenomenon even at high Ba^{2+} concentrations. It means that this method of Ba^{2+} incorporation into KTA structure is unlikely. The $KAsO^{2+}$ replacement by Ba^{2+} is also hardly probable since two oxygen vacancies would be created for each Ba^{2+} ion. The latter would promote polydomain character of KTA samples, which was not observed in experiment. Besides, both above mentioned versions are unlikely because they are associated with K and As vacancies, which are present already in high concentrations in the melt.

Thus, $2Ba^{2+}$ incorporation in KTA is probably connected with K_2TiO^{4+} replacement and TiO^{2+} vacancies formation. In this case only one oxygen vacancy is created, and as such $Ba^{2+} \rightarrow K$ replacement will result in domain generation in the minimum extent. It is necessary to note that titanium concentration in the melt is considerably less than that of potassium and arsenic. Thus TiO^{2+} vacancy creation is the most probable.

Let us discuss the K^+ replacement by trivalent ions. It has been shown that In^{3+} replaces K^+ and Ti vacancies. Thus a charge compensation of $In^{3+} \rightarrow KTiO^{3+}$ substitution is associated with TiO^{2+} defect as in the case of Ba^{2+}. However, the In^{3+} incorporation coefficient in KTA,

from the melt estimated as ([In] in KTA) / ([In] in melt) is equal to 0.01, which is 20 times lower than for Ba^{2+}. The low value for coefficient of K^+ replacement by In^{3+} could be explained by three reasons:

1. The structure instability of K^+_1 and X chains relative to K^+_2 and Y chains has already been mentioned. There are two TiO_6 octahedrons of X chains near K^+_1, and a little further an octahedron of Y chain is located. Thus it is not surprising that TiO vacancy is created in a stressed X chain, and a K^+_1, located near a vacancy, is replaced by In^{3+}. The creation of a vacancy in the Y chain and replacement of stable K^+_2 by In^{3+} does not occur.
2. The most probable reason is that the initial step in K^+ replacement by In^{3+} is namely formation of a TiO^{2+} vacancy with further trivalent negative charge compensation which substitutes for K^+. The initial K^+ replacement by In^{3+} with a promotion of a TiO^{2+} vacancy near by is not likely to occur.
3. Detailed charge compensation is important at $KTiO^{3+}$ replacement by In^{3+}. Components of an indium- vacancy pair are located close to each other, and the charge is compensated in a local area and does not affect the further KTA growth and unit cell defects.

In the case of K^+ replacement by Ba^{2+} the situation differs from the previous case. The very important circumstance is an absence of detail charge compensation at K_2TiO^{4+} replacement by $2Ba^{4+}$. Let us suppose that a TiO^{2+} vacancy was formed in the X chain during KTA growth. Ba^{2+} replaces K^+_1 which located near vacancy, but it does not compensate the surplus negative charge. For complete compensation the second $Ba^{2+} \rightarrow K^+$ replacement is also necessary. But all potassium ions which could be replaced by Ba^{2+} are at larger distances from the vacancy than the first K^+ ion. As a result compensation, of a negative charge by two Ba^{2+} is not of a local type. The adjacent Ba vacancy pair has a negative charge which can promote replacement of the adjacent K^+ by Ba^{2+}. A remote Ba^{2+} carries a surplus positive charge which can promote a new TiO vacancy quite near it. Namely the absence of compensation can be the reason for a large Ba^{2+} introduction coefficient into KTA.

It can be noted that the above mentioned hypothesis is confirmed indirectly by a large coefficient of Li^+ replacement by Nd^{3+} in $LiNbO_3$ and $LiTaO_3$. The most probable charge compensation is as $4Nd^{3+} \rightarrow 3LiNbO^{4+}$. It means that charge compensation is also absent here, which brings a high Nd^{3+} incorporation coefficient in $LiNbO_3$ and $LiTaO_3$. The other type of compensation as $Nd^{3+} \rightarrow Ti_2NbO_2^{3+}$ is unlikely since it brings the appearance of a Li vacancy and two oxygen vacancies for one Nd ion. It could distort strongly the $LiNbO_3$ lattice, which is not observed in experiments.

The high substitution coefficients for Se^{3+} (as 0.77 at low Se concentration in the melt) and for Fe^{3+} (0.54 at low Fe content in the melt) in KTA were found. These values may be unambiguously explained by replacement of not only K^+, but also of Ti^{4+} by Se^{3+} and Fe^{3+}. Fe^{3+} as well as Ti^{4+} are transitional ions and this radius slightly exceeds the Ti^{4+} ionic radius. The Ti^{4+} replacement by Fe^{3+} results in appearance of a surplus negative charge, which involves K^+ replacement by Fe^{3+}. But in this case the surplus positive charge appears, which promotes TiO^{2+} vacancy generation. The latter results in a negative charge which involves a new $Fe^{3+} \rightarrow Ti^{4+}$ replacement with charge compensation or promotes a new $Fe^{3+} \rightarrow K^+$ change with creation of surplus positive charge.

The Se^{3+} is the nearest neighbor of Ti^{4+} on the Periodic Table (system). Its ionic radius is larger than that of Ti^{4+}, but is smaller or equal (according to various tables of ionic radii) to the ionic radius of Zr^{4+}. In the previous report we showed that Zr^{4+} replaces Ti^{4+} with a coefficient of ~1. Thus it is clear that as in the case of Fe^{3+} there will be a situation of absence of charge compensation which is supposed to result in large Se^{3+} incorporation coefficient properties which differ strongly from those of Ti. Thus the Ti^{4+} replacement by In^{3+} does not occur. Nd^{3+} has a large ionic radius relative to In^{3+}. It is the reason why Nd^{3+} cannot replace Ti^{4+}. Hence the $Nd^{3+} \rightarrow K^+$ replacement coefficient would be lower or equal to that for $In^{3+} \rightarrow K^+$ replacement, which is small.

From the above it is clear that to increase the Nd^{3+} incorporation coefficient the modification of KTA structure is necessary. The following directions in this work can be singled out:

1. To replace K or Ti by isovalent ions of larger radius which is supposed to increase the imperfection of KTA structure and the size of the Z-pore. Both ways are expected to result in an increase of Nd^{3+} incorporation coefficient into KTA.
2. To replace K^{+}_{I}, Ti^{4+}, As^{5+} or their groups, including those with oxygen participation, by cations of various valences in order to generate point defects with negative or positive surplus charge in the lattice.

The positive centers are expected to promote a TiO^{2+} vacancy generation which involves Nd^{3+} incorporation instead of K near this vacancy. The negative center also promotes Nd incorporation into KTA lattice.

During this effort several interesting results were obtained. Figure 4 shows the enhanced transmission in the infrared when KTA is doped with Zr, Hf, and Ba. The heavy metal dopant appear to dampen the vibrational state of the AsO_4 bonds moving the absorption bond further into the infrared.

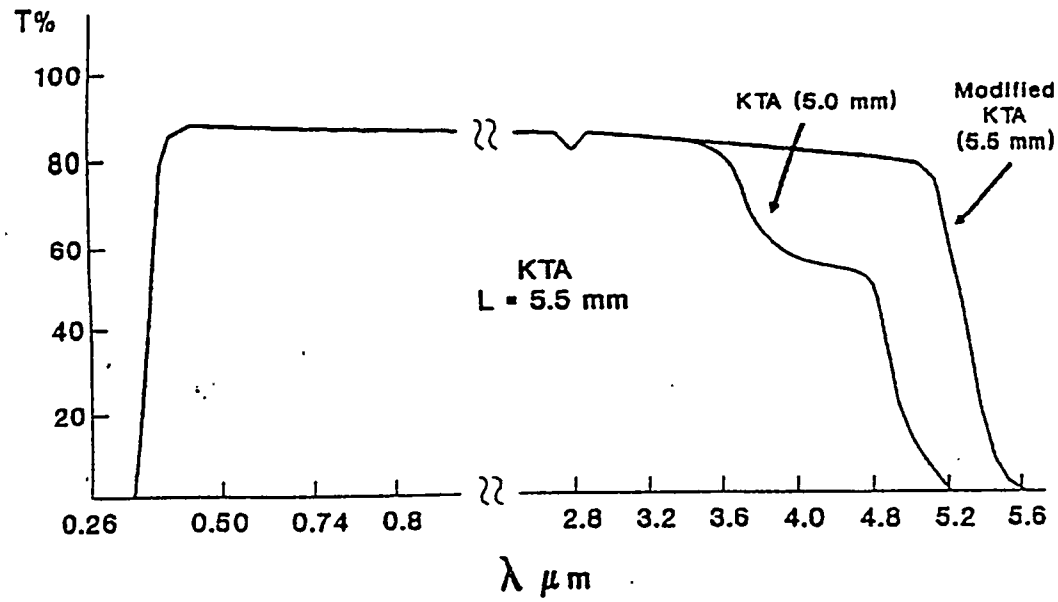

Figure 4. KTA transmission spectra

Figure 5 shows the effusion spectra of Nd:Ba:KTA. This effort has also resulted in determining that certain metal complexes increase the nonlinear coefficient of KTA, and that the line shape of the Nd can be tailored to some degree.

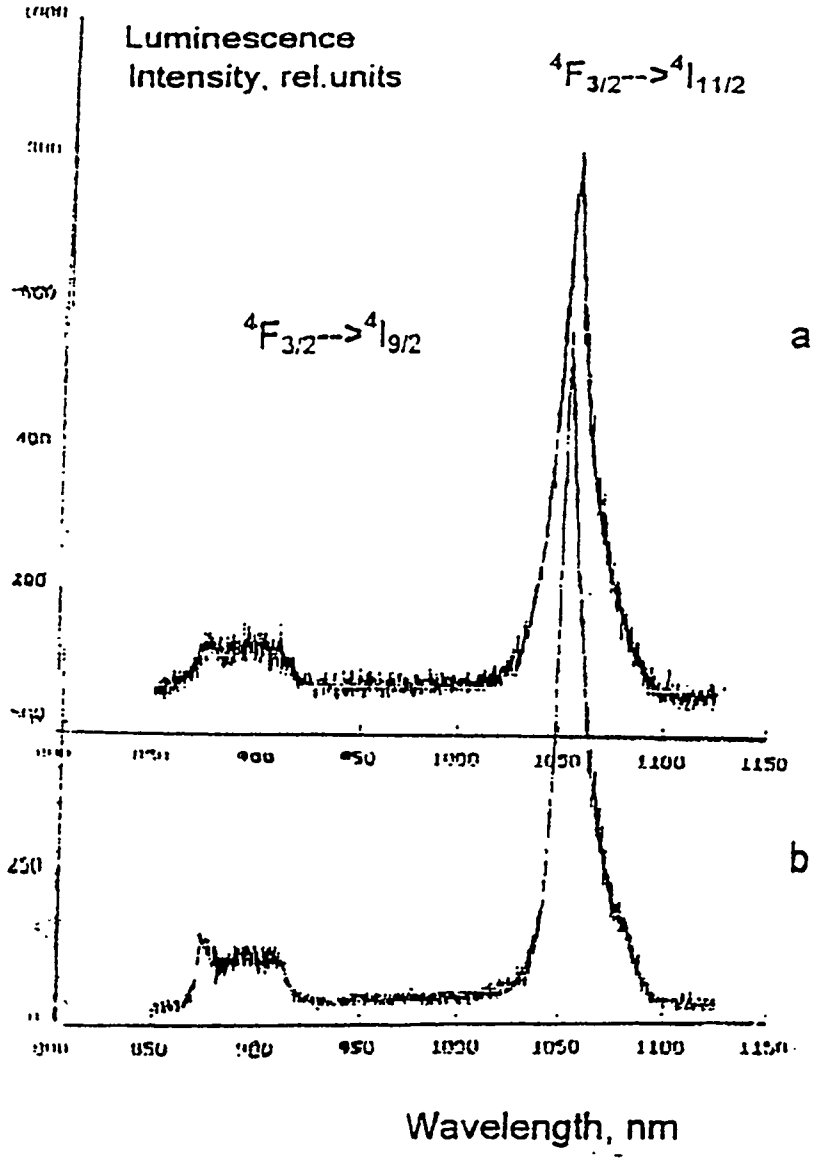

Figure 5. Nd^{3+} emission of Nd:Ba:KTA at 300°K (a) and 80°K (b)

Neodymium doped levels were approximately 0.1%, which is too low for efficient laser operation. Figures 6 and 7 illustrate the absorption and emission of Yb:KTA respectively. The stimulated emission cross-section is 2.9×10^{-19} cm^2, which is very good. Dopant levels of ytterbium were approximately 1.0%. Pumping may be possible with 965 nm laser diodes, but the emission and absorption lines overlap so that spontaneous re-absorption may be a problem at room temperature

with broad band laser mirrors. However, by using a very narrow laser coupling optic at 975 nm, Yb:KTA should lase.

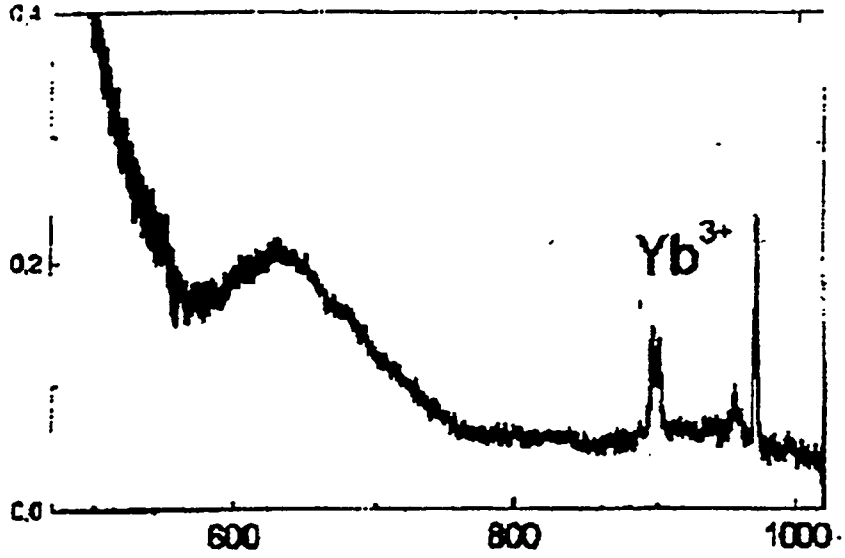

Figure 6. Absorption spectrum of Yb:KTA (80 K)

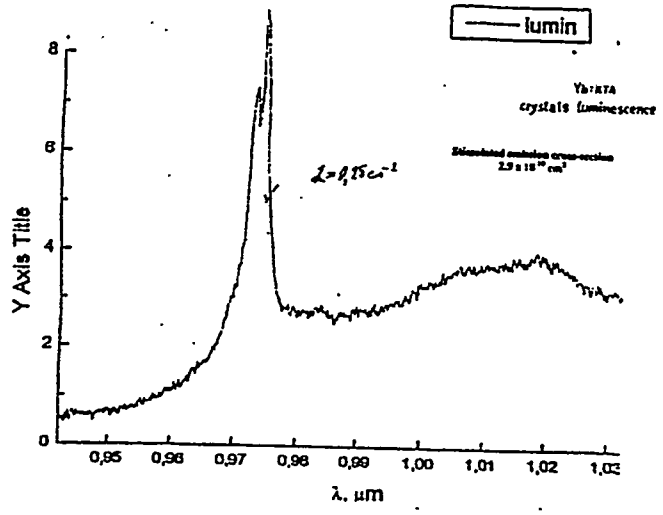

Figure 7. Yb:KTA emission spectra

Experiments evaluating Yb:KTA spontaneous fluorescence indicate that at the current Yb doping levels, a gain length of 1.5 cm will be required. Crystals of Yb:KTA of a size of 5 mm x 5

mm × 15 mm have been produced and cut. Currently these crystals are being polished and coated for lasing experiments.

VI. No inventions have been disclosed or reported.

VII. Commercialization

The production of enhanced mid-infrared transmission KTA will find use in optical parametric oscillators. Such devices will be utilized in laser remote sensors for measuring light hydrocarbons and volatile organics in the 3.0 μm region. Production of crystals with lengths of 15 mm are comparable to production in the United States. LaSen, Inc. is collaborating with Big Sky Laser to test and incorporate these crystals into an intracavity OPO for use in a fixed site laser monitor.

Until laser tests are done, the usefulness of Yb:KTA is as yet undetermined. However, given the high stimulated cross-section and a narrowing of the absorption/emission lines by metal co-doping self doubling (975 nm → 487 nm) could find uses in medical applications and in military systems requiring penetration through sea water. Self OPOing (OPOL) operation would find use in infrared remote sensors and infrared surgical systems.

One manufacturing issue that must be addressed is a routine test to evaluate the microdomaining structure of the crystals early in the fabrication process. This will lower the cost of the crystals and decrease delivery times.

VIII. Future Collaboration

Currently LaSen, Inc. is collaborating with Znanie Ltd. to refine a co-metal mix of Yb:Nd:KTA and Yb:Cr:KTA in an attempt to decrease the spontaneous re-absorption of lasing photons.

LaSen, Inc. is also working to fund a large aperture, periodically poled lithium niobate crystal program. At this time, LaSen, Inc. and Znanie Ltd. are discussing technical tasking and costing.

LaSen, Inc. is also working with Znanie Ltd. and the US State Department of SABIT program to employ a solid-state physicist/chemist with expertise in semiconductor oxide materials.

IX. Conclusions

The production and testing of a laser crystals program was succcessful in producing large (5 mm × 5 mm × 15 mm) co-doped KTA crystals. These crystals have been co-doped with Ba, Zr and Hf to produce enhanced transmission in the 3.6 - 5.1 μm region. These crystals have now been ordered commercially for lidar remote sensor systems.

KTA has been doped with neodymium, erbium, holmium, thulium, and ytterbium. Evaluation of these crystals are continuing. Yb:KTA appears to be the best candidate as a lasing material with a dopant level of 1.0%, and a stimulated cross-section of $\approx 3 \times 10^{-19}$ cm^2.

KTP/KTA analogs of tellurium and antimony do not produce crystalline structures that have nonlinear optical properties suitable for second harmonic generation or parametric processes.

Collaboration continues on co-doped metals in KTA and advanced crystal projects involving $LiNbO_3$ and semi-conductor oxides is being explored.

Distribution

Tom Schmidt, MS-6273, 4500-N
Chris Valentine, MS-8242, 701SCA
Ray Ford, MS-8084, 9203
DOE/ORO, FOB, Room G-209
Joyce Shepherd, MS-6416, 5002
P. L. Gorman, MS-6229, 4500-N
Lab Records, MS-6285, 4500-N
Y-12 Central Files, MS-8169, 9711-5 (3 copies)

Allen R. Geiger, LaSen, Inc., 300 N. Telshor, Suite 600, Las Cruces, NM 88001 (5 copies)